13

Influence of barium adsorption on the work function of hafnium grids cathode-grid assembly

© O.E. Glukhova,[1,2,3] D.A. Kolosov,[1,3] V.I. Shesterkin,[3] T.M. Krachkovskaya,[3] S.D. Zhuravlev,[3] R.Yu. Bogachev[3]

[1]Saratov National Research State University,
410012 Saratov, Russia
[2]I.M. Sechenov First Moscow State Medical University,
119048 Moscow, Russia
[3]Joint Stock Company Research and Production Enterprise „Almaz“,
410033 Saratov, Russia
e-mail: kolosovda@bk.ru

Received June 6, 2024
Revised July 26, 2024
Accepted July 31, 2024

The interaction of barium atoms with the surface of a hafnium grid located near the emitting surface of a metal-porous cathode is studied. The type of crystal lattice and the surface structure of hafnium used as a material for grid structures in cathode-grid units of vacuum tubes are determined using X-ray phase analysis. The adsorption of barium atoms on the surface of hafnium at the operating temperature of the cathode — 1080°C — is studied using the density functional method with molecular dynamics. It is found that the first adsorbed layers of barium atoms are introduced into the crystal lattice of hafnium and increase the work function of electrons. After saturation of the near-surface layer of hafnium, barium atoms accumulate on the surface, forming a crystalline film. During its formation, the work function of the film decreases and, starting from the twentieth layer, stabilizes at the value of the work function of barium.

Keywords: density functional theory, desorption, adsorption, molecular dynamics modeling, dispenser cathode, grid electrodes.

DOI: 10.61011/TP.2024.10.59369.200-24

Introduction

Single (current-intercepting) or double (non-current-intercepting) grid structures are used for low-voltage control of the electron beam current in pulsed vacuum tubes [1]. In double structures, the shadow grid is positioned between the emitting surface of the cathode and the control grid so that its wires screen the wires of the control grid from intercepting the cathode current directly. Weak thermionic emission from grids heated to a high temperature is one of the key requirements imposed on grid structures. Their structural material should have fine anti-emission properties, which may be provided by a high work function and chemical inertness [2]. In normal operation, grid structures interact with products evaporating from the surface of a dispenser cathode (DC) impregnated with an active substance (e.g., barium and calcium aluminosilicate with a ratio of $3BaO{:}0.5CaO{:}0.5SiO_2{:}1Al_2O_3$). The range of temperatures of the emitting DC surface in a device in operation is 1080−1150°C. These are the conditions in which the processes of adsorption of the active substance on the surface of grid wires and its desorption proceed simultaneously. Desorption intensifies with increasing temperature and depends on the binding energy of the sorbate with the sorbent. At temperatures of 500−600°C under a vacuum of $\sim 10^{-7}$ Torr, molecules adsorbed at lower temperatures are desorbed completely. At higher temperatures, adsorbed atoms and molecules may form stable chemical bonds with the surface and penetrate into the material. In view of this, the selection of grid materials with high work function and melting temperature values is not a necessary and sufficient condition for their use with the object of reducing parasitic thermionic emission. For example, hafnium grids with an electronic work function of 3.5 eV are chosen for the fact that the thermionic emission current from such grids interacting with the DC evaporation products at a temperature of 800°C is approximately 28 times lower than the thermionic emission current from molybdenum grids with a work function of 4.5 eV [2,3].

The emitting DC surface is coated with a Os−Ir−Al composite film $\sim 0.35\,\mu$m in thickness to reduce the work function and the rate of evaporation of the active substance. The primary products of DC evaporation are Ba ($\sim 90\%$) reduced in chemical interaction of barium oxide with a tungsten sponge [4] and BaO ($\sim 9\%$). This ratio is due to the difference in their melting points: ~ 730°C for Ba and ~ 1930°C for BaO [5]. The results of analysis of the chemical composition of the surface of grids removed from devices after 100 h of operation revealed that the surface of shadow grid wires (grid facing the emitting surface of the cathode) is coated with a film up to $0.3-0.5\,\mu$ in thickness, which contains barium (46%) and calcium (7.3%). This ratio of the indicated elements corresponds to their percentage in aluminosilicate. The low calcium

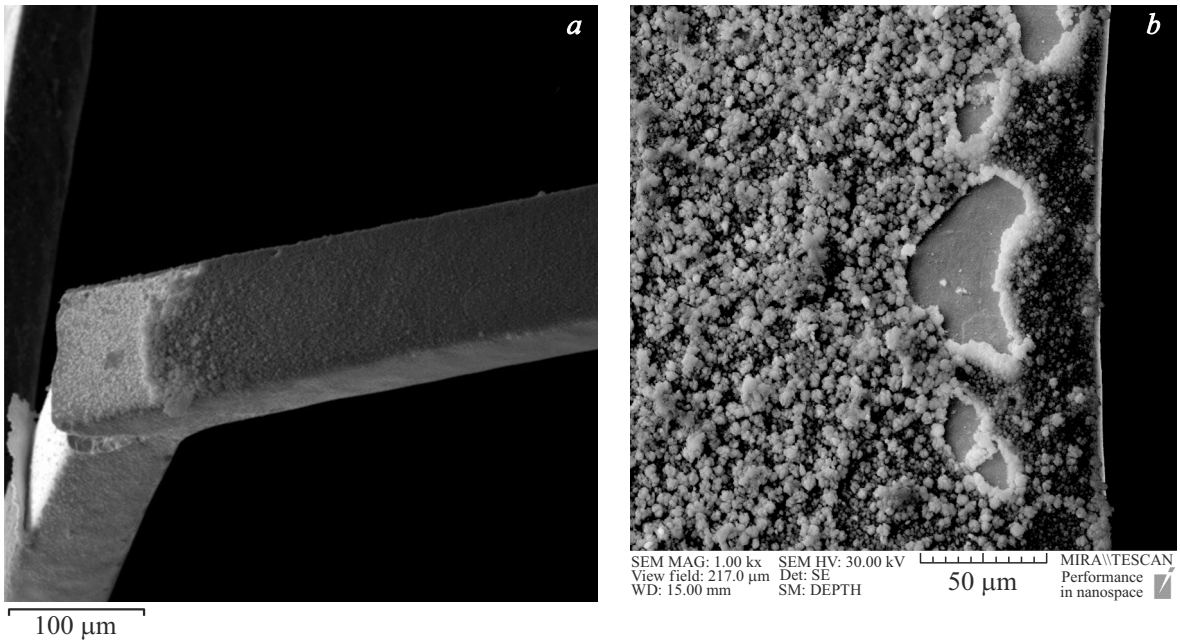

Figure 1. Film of the active substance delaminating from a shadow grid wire (a) and peripheral fragment of the shadow grid (b).

content determined for the grid may be attributed to its melting point of $\sim 840^\circ$C, which is 140°C higher than that of barium. The control grid temperature at a cathode temperature of 1080°C is $\sim 780^\circ$C, which is above the melting point of barium. Osmium and iridium were not detected on the surface of grids, since they have high melting points (3033 and 2465°C, respectively).

Thus, the thermionic emission current from Hf grids is governed by the work function of the surface with the DC evaporation products adsorbed on it. To analyze thermionic emission from a grid and find a way to suppress it, one needs to know not only the percentage of elements adsorbed on its surface, but also the binding energy of individual atoms and atomic layers deposited onto the grid in the course of operation of the cathode and their effect on the electronic work function of the grid. Since 90% of the active substance evaporated from the cathode surface is barium, the mechanism of interaction of barium with the surface of pure hafnium at high temperatures (800−1300°C) and the mechanisms of adsorption and desorption of barium were investigated in the present study. Since sheet hafnium used in grid fabrication has a predominantly hexagonal crystal lattice structure (partially triclinic), calculations were performed for a hexagonal lattice.

1. Chemical composition of the active substance adsorbed on the grid

It was established that the cathode-facing and lateral surfaces of shadow grid wires are coated with a homogeneous active substance film consisting of barium and calcium with a weight content (averaged over the grid surface) of 40 and 6%, respectively. Since barium is the primary product of evaporation from the cathode (90%), modeling was performed only for this element. A delaminating film of adsorbed substances with a thickness up to 0.35 μm is seen at the point of wire fracture. The film had a non-uniform loose structure in the periphery beyond the radial wires (Fig. 1, b). Small amounts of barium ($\sim 0.7\%$) and calcium ($\sim 0.2\%$) were detected on the shadow grid surface facing the anode,. Small amounts of barium (0.23%) and calcium (0.21%) were detected on the cathode-facing surface of control grid wires. Neither barium nor calcium were found on the reverse (anode-facing) side of the control grid.

2. X-ray phase analysis of the crystal lattice of hafnium

X-ray phase analysis of the hafnium grid blank was carried out using a DRON-8T multifunctional X-ray diffractometer with the software supplied by the manufacturer (JSC Bourevestnik, Russia), the PDF-2 database version 2.2102 (International Centre for Diffraction Data, United States, 2021) [6], and Crystallography Open Database [7]. To refine the structural parameters of major and impurity phases, the full profile of X-ray diffraction patterns was analyzed using the Rietveld method in FullProf Suite [8]. The following parameters were varied: scale factor, coefficients of the equation for background approximation, zero shift, parameters of crystal structures, phase content, profile parameters, and texture parameters for the major phase.

It was determined that the crystalline phase for the studied samples is textured hexagonal hafnium (α-Hf). Its lattice cell is shown in Fig. 2. The cell dimensions are

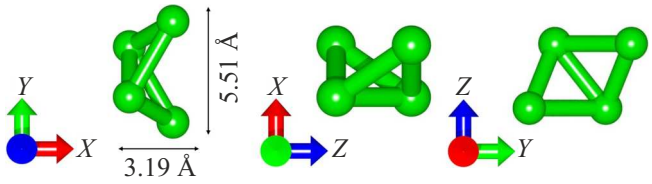

Figure 2. Crystal structure of α-Hf.

also indicated there. In addition, it was established that the hafnium surface is characterized by Miller index (002).

3. Calculation procedure

The atomistic structure and electronic properties were examined using density functional theory (DFT) with the Perdew–Burke–Ernzerhof (PBE) generalized gradient approximation (GGA) implemented in the SIESTA 4.1.5 software package [9,10]. Optimization (geometric relaxation) was performed to obtain an equilibrium configuration of lattice cells (supercells). This was achieved by solving the minimax problem with the aim of identifying the global minimum of total energy by varying the coordinates of all atoms and the lengths of translation vectors. A split-valence double-zeta plus polarization (DZP) basis set was used. The Monkhorst–Pack scheme was applied to construct a grid of k-points and partition the reciprocal space. The atomic structure was optimized with an accuracy of 0.04 eV/Å for interatomic forces and with an accuracy of 10^{-5} eV in total energy. The global minimum of total energy was identified using the Broyden–Pulay algorithm. The first Brillouin zone was characterized by a $10 \times 4 \times 1$ grid. The cutoff of the real spatial grid was wet to 600 Ry in all calculations, which corresponds to a resolution of approximately 0.06 Å^3. All calculations of the electronic structure and electronic work function were carried out with preliminary optimization of the lattice cell, which took anywhere from several hours to several days. The distribution of the electron charge density over atoms was determined in accordance with the Mulliken population analysis. Modeling of the studied system at different temperatures was performed within the Born–Oppenheimer quantum molecular dynamics approximation. The trajectories of all atoms were calculated within a given period of time with a time step of 0.1 fs.

The work function of electrons emitted by the surface of a quasi-2D sample into vacuum was calculated as

$$\Phi = E_{vac} - E_F, \tag{1}$$

where E_{vac} is the energy of an electron, which has escaped from a solid-state structure into vacuum, near the surface of this structure and E_F is the Fermi energy of the solid-state structure. A number of papers focused on calculating the energy barrier for electron escape into vacuum and the electron energy in vacuum in close proximity to the surface have already been published. The values of E_F and E_{vac} for the examined structures were calculated in the present study. An important point in such calculations was the determination of energy E_{vac} of an electron that has escaped from the structure and still remains in close proximity to the surface. The calculation of this energy was preceded by the calculation, within a self-consistent field, of potential energy (potential) profile $V_{SCF}(z)$ of an electron „moving" from the quasi-2D sample lattice into vacuum and crossing atomic planes on its way. Here, z is the axis perpendicular to the surface of the sample being studied. Averaging was performed to determine the position of central reference point of potential $V_{SCF}(z)$ on axis Z:

$$V_{SCF}(z) = \frac{1}{d} \int_{z-d/2}^{z+d/2} V_{SCF}(z')dz', \tag{2}$$

where d is the quasi-2D sample thickness. Potential $V_{SCF}(z)$ is the solution of the electrostatic Poisson equation for a self-consistent field with account for the contribution of all ionic cores of the atomic lattice. Potential $V_{SCF}(z)$ at a given coordinate z was averaged within each atomic plane over all atoms of the supercell of this plane. The interplanar potential was averaged along z.

4. Results

4.1. Work function and interaction energy

The optimum hafnium film thickness (i.e., the optimum number of layers with each of them being a lattice cell) was established first. Optimality was understood as the correspondence of key emission parameters of the quasi-2D structure to similar parameters of bulk samples, since this ensured physical validity of the results of studies for quasi-2D structures. Thus, ten supercells with the number of elementary cells varying from 1 to 10 (along axis Z) were constructed; their optimization was carried out; and Fermi energy E_F, electron energy in vacuum E_{vac}, and the work function were calculated. Figure 3, *a* shows three views of the lattice cell and a monolayer fragment. The Hf–Hf bond length in the monolayer was 3.2 Å, and the thickness was 2.4 Å. The vectors of translation along axes X and Y are 3.191 and 5.531 Å respectively. The calculated values of the work function at a temperature of 300 K for layered films are presented in Fig. 3, *b*. It can be seen that the work function decreases from ~ 4.24 to 4.15 eV as the number of hafnium layers in the film increases.

The work function decreases rapidly with an increase in layer number, eventually reaching saturation. In the present case, saturation is observed starting from the sixth layer of hafnium. As was demonstrated above, the work function is the sum of two energy quantities: Fermi energy E_F and energy E_{vac} of and electron that has escaped from the structure. Figure 3, *c* shows the profile of E_{vac} variation for a ten-layer film. This is the energy of an electron moving through atomic planes into vacuum. It decreases in each

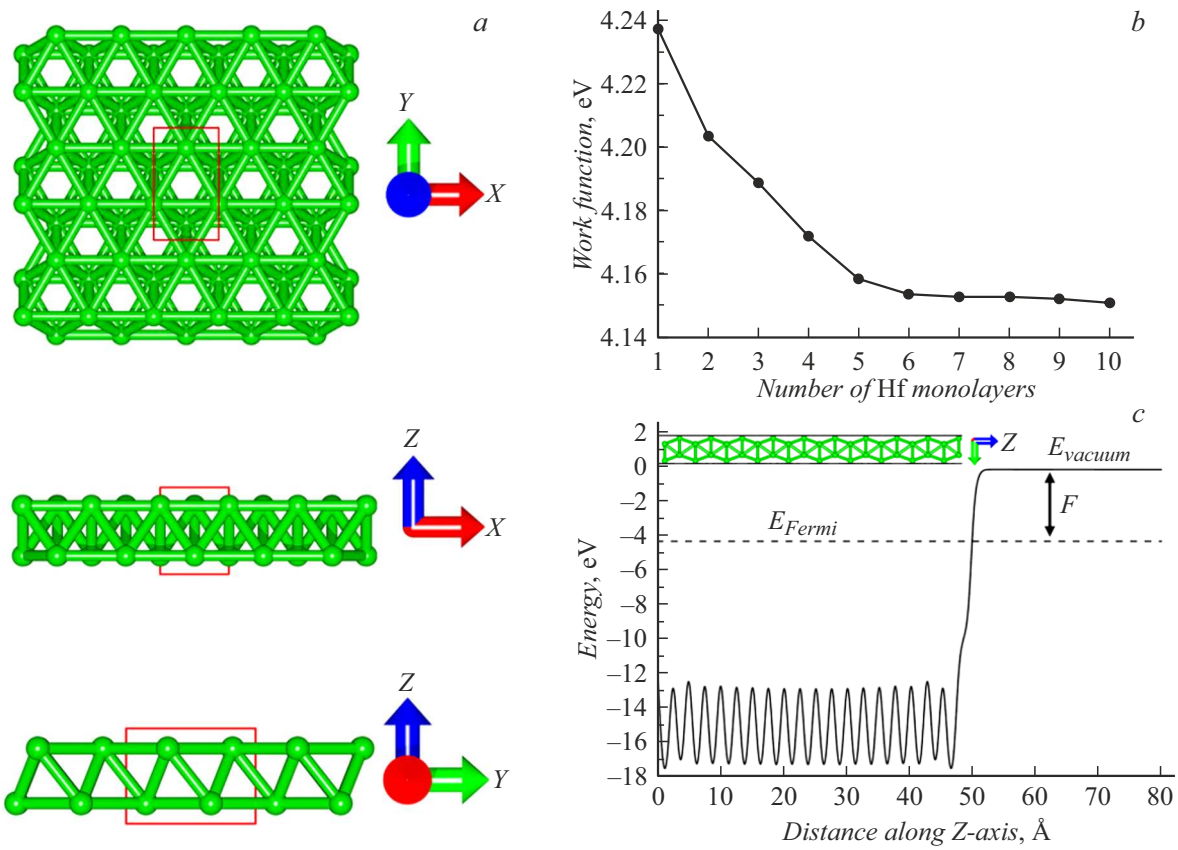

Figure 3. Lattice cell of hexagonal hafnium (a), work function of layered hexagonal hafnium (b), and variation of energy E_{vac} for a ten-layer film (c).

atomic plane and increases slightly in the interplanar space (i.e., oscillates). When the last atomic layer is crossed, the energy increases rapidly to a value close to zero. Figure 3 c demonstrates that energy E_{vac} is non-zero (several tenths of an electronvolt below zero). As the number of layers grows, the Fermi energy decreases from -4.15 to -4.37 eV; the energy of an electron in vacuum also decreases from -0.01 to -0.217 eV.

Owing to the complexity of calculations, the case of five hafnium layers was chosen as the main supercell for examining the adsorption of barium, since the work function of hafnium ceases to vary in any significant way when this number of layers is reached.

4.2. Adsorption of barium on the surface of hexagonal hafnium

The process of barium adsorption was studied via quantum molecular dynamics (MD) annealing simulations in SIESTA 4.1.5. The temperature in calculation was maintained at 800°C. The first Brillouin zone was characterized by a $10 \times 4 \times 1$ Monkhorst–Pack grid. The annealing time was 1000 fs with a step of 0.1 fs. Each barium layer was deposited in two stages:

(1) deposition of barium atoms with subsequent relaxation;

(2) initiation of annealing MD simulations following the end of relaxation.

The work function was determined after MD calculations. Figures 4, a–f present snapshots of the MD calculation and diffusion of barium atoms deeper into the hexagonal hafnium lattice. The variation of binding energy of the Hf/Ba system in the process of barium diffusion into the crystal lattice of hafnium is illustrated in Fig. 4, g. The binding energy was calculated in the following way:

$$E_{connect\,\mathrm{Hf+Ba}} = E_{\mathrm{Hf+Ba}} - (E_{\mathrm{Hf}} + E_{\mathrm{Ba}})/n_{\mathrm{Hf+Ba}}, \qquad (3)$$

where $E_{\mathrm{Hf+Ba}}$ is the total energy of the Hf + Ba structure (Figs. 4, a–f), E_{Hf} is the total energy of a pure hafnium film (without barium atoms), E_{Ba} is the total energy of a single barium atom, and $n_{\mathrm{Hf+Ba}}$ is the total number of hafnium and barium atoms in a supercell. It is worth noting that the supercell in Figs. 4, a–f was translated along axis Y for clarity. Calculations were performed for a five-layer hafnium supercell with one barium atom (21 atoms in the system); i.e., a cell with five hafnium layers and one barium atom was examined. Hafnium and barium atoms are colored green and pink, respectively.

The MD calculation demonstrates that, from 200 fs onward, barium atoms diffuse deeper into the hafnium lattice, altering its crystal structure on the surface. The

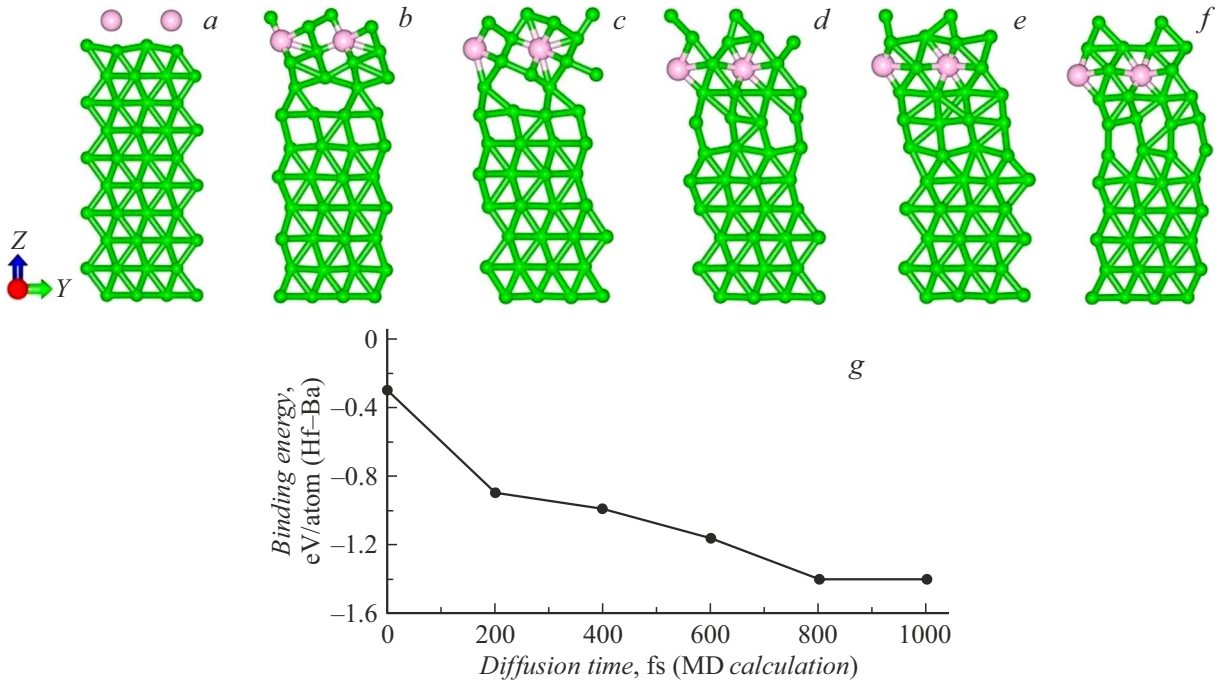

Figure 4. Snapshots of the MD calculation. Binding energies of the first barium layer at the zeroth MD step (*a*); 200 fs (*b*), 400 fs (*c*), 600 fs (*d*), 800 fs (*e*), and 1000 fs (*f*) after the start of MD calculations; and plotted variation of the Ba–Hf binding energy in the process of barium diffusion into the crystal lattice of hafnium (*g*).

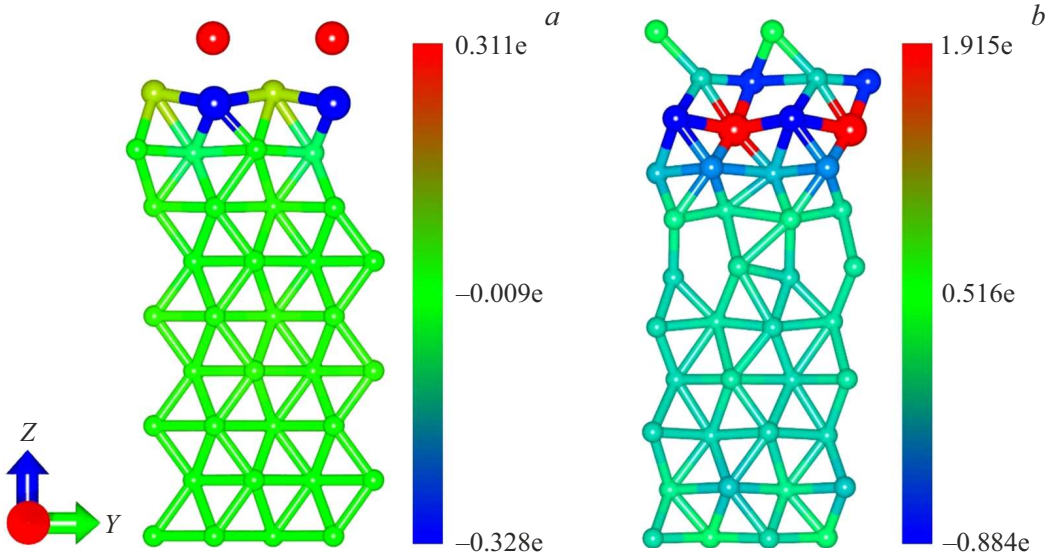

Figure 5. Pattern of charge redistribution between barium and hafnium atoms at the zeroth MD step (*a*) and after 1000 fs (*b*).

penetration depth ceases to change significantly after 600 fs, reaching approximately 5 Å. The binding energy of barium with hafnium was −0.29 eV/atom (Hf–Ba) at the zeroth MD step, but then increased significantly to −1.4 eV/atom (Hf–Ba), which indicates that diffusion is energetically favorable in this system. Further diffusion of barium into the crystal was hampered by the lower layers of hafnium: their positions remained virtually unchanged throughout the entire duration of MD calculations. It is worth noting that, according to the experimental data from [5], the depth of penetration of barium into the crystal lattice of hafnium is several tens of nanometers. With a hafnium grid thickness of several hundred or thousand of micrometers, nanometer defects on its surface do not exert any significant influence on the strength properties of the grid.

Figure 5 illustrates the redistribution of charge over the supercell atoms at the time points of 0 and 1000 fs in the MD calculation.

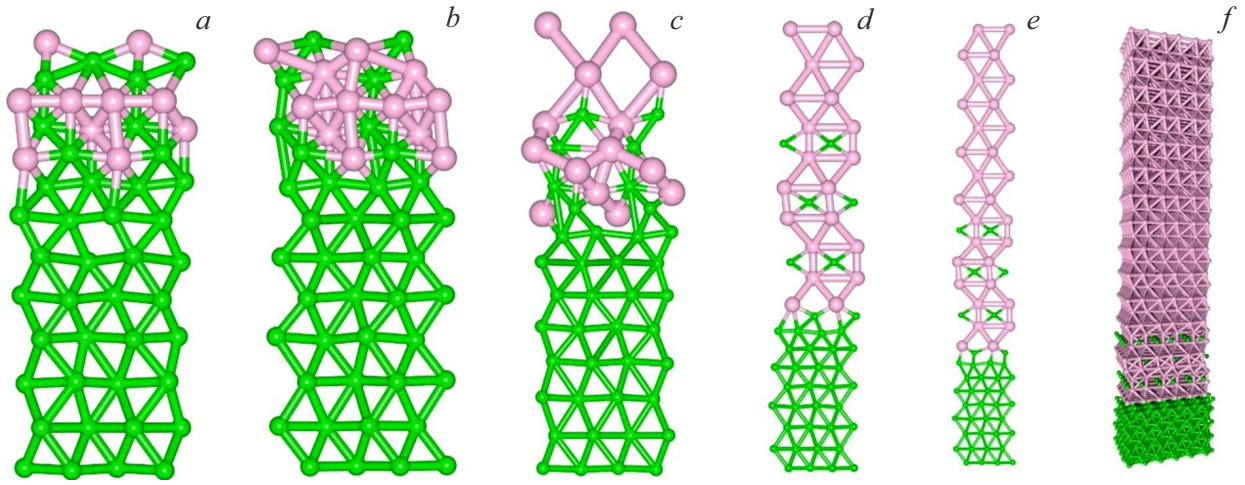

Figure 6. Deposition of five (*a*), six (*b*), seven (*c*), ten (*d*), fifteen (*e*), and thirty (*f*) layers of barium atoms onto the surface of a hafnium crystal.

According to the Pauling electronegativity scale, barium and hafnium have an electronegativity of 0.89 and 1.3 [11,12], respectively, which enables partial transfer of the charge from barium to a hafnium atom. The following is seen in Fig. 5: at the initial MD stage (zeroth step), the barium atom transferred 0.311 electrons to the hafnium crystal, becoming a positively charged ion. The transfer of 0.311 electrons does not imply „division" of an electron; instead, electron clouds of the Ba−Hf system redistribute toward an increase in the electron density of hafnium at the expense of the electron density of barium. It is also worth noting that the Ba−Hf system as a whole is electrically neutral. Let us return to the case of barium diffusion into the hafnium lattice (Figs. 4, *a*–*f*). The atomic radii of hafnium and barium atoms differ fairly widely: 224 pm for barium and 159 pm for hafnium, which should translate into a rather weak barium diffusion. However, a considerable transfer of charge is observed when barium interacts with hafnium (see Fig. 5), and the greater this transfer is, the deeper the barium atom penetrates into the hafnium lattice. The reason for lowering of the diffusion barrier is the reduction in radius of the barium atom due to it becoming a positive barium ion. According to [13], the Pauling empirical crystal radius for a barium +2 ion is 135 pm, which is fairly close to the hafnium atom radius. It is worth noting that the upper layers of hafnium also enter an ionic state, but the excess negative charge is redistributed throughout the entire crystal lattice.

As part of investigation of the process of barium diffusion into the crystal lattice of quasi-2D hafnium, MD studies with a gradual increase in the number of barium layers on the surface of hexagonal hafnium were performed next. Thirty layers of barium were deposited onto the surface of hafnium. Figure 6 illustrates the cases of 5, 6, 7, 10, 15, and 30 barium layers.

As the number of barium atoms on the surface of quasi-2D hafnium increased, gradual formation of a barium crystal was observed. Figures 6, *a*–*c* illustrate the process of formation of a barium crystal on the surface of a hafnium crystal. It can be seen that barium atoms diffuse only to a certain depth within hafnium layers, thus revealing „saturation" of the hafnium film with barium atoms. This saturation effect was observed while barium atoms penetrated into hafnium with certain hafnium atoms still remaining on the surface (Fig. 6, *b*). Barium atoms then stop diffusing deeper into the hafnium film and start forming their own crystal on the film surface (Fig. 6, *c*). As the number of barium layers on the surface increases, hafnium atoms of the upper layers, in turn, begin to diffuse into the formed barium crystal (see Figs. 6, *d, e*). Figure 6, *f* presents an extended supercell with thirty layers of barium on the hafnium film surface. It can also be seen that hafnium atoms have penetrated only the first few layers of barium.

The overall time of the MD study with the diffusion of barium into the hafnium film taken into account was 30 ps (30 000 fs); the work function was calculated for each added layer. Figure 7 presents the obtained plot of the dependence of the work function on the number of barium layers in the structure. The work function increases as the first six layers of barium diffusing into hafnium get deposited. In fact, a new composite material is being formed. The presence of even 1−2 hafnium layers over barium raises the work function from 4.15 to 4.9 eV. When the seventh layer of barium atoms is deposited, the work function decreases sharply, since it is governed by barium from this point on. With the 23rd layer of barium deposited, the work function of the structure reaches a plateau at approximately 3.75 eV. This work function value is typical of pure crystalline barium (3.74 eV) in the chosen DZP basis and is achieved already with 20 layers of barium present on the hafnium surface.

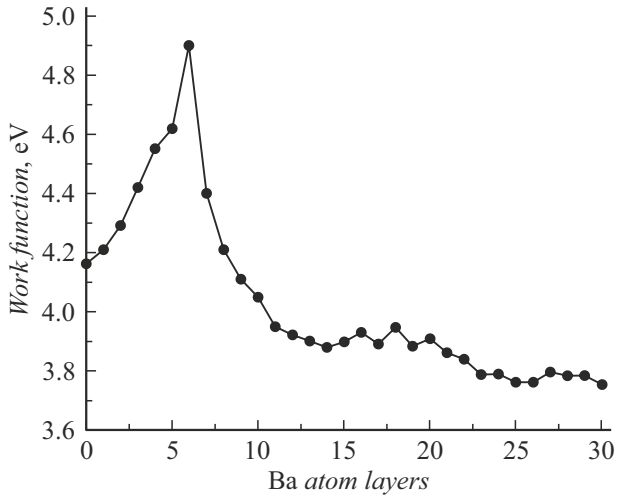

Figure 7. Dependence of the work function on the number of barium layers.

It is fair to say that the barium–hafnium composite material with 7–30 Ba layers behaves, on the whole, like a barium crystal and does not „feel" the hafnium film. The obtained results agree closely with the data presented in [14], where the effect of diffusion of barium atoms deeper into the hafnium film with a subsequent work function reduction was noted.

4.3. Desorption of barium from the surface of hexagonal hafnium

To induce desorption of the DC evaporation products from the hafnium surface, the control grid is treated by applying power (i.e., by additional heating to 1300°C) . The case with seven layers of barium on the hafnium surface and the case of a pure hafnium crystal lattice were considered in the process of examination of barium desorption. In calculations, the supercell was expanded along the X and Y axes. Figure 8 presents different scenarios of desorption of a barium atom: from a barium lattice, from the surface of a barium lattice, from a pure hafnium lattice, and from a pure hafnium lattice in the presence of a second barium atom. In each of these cases, the Ba–Hf binding energy was calculated using the method of gradual detachment: the barium atom was shifted in the direction of axis Z toward the vacuum region in steps of 0.25 ÅThe binding energy was calculated by formula (3) at each step. From the energy standpoint, the distance of detachment of the barium atom was 5 Å.

Figure 9 presents the dependences of the binding energy on distance to the lattice.

The origin points of these curves correspond to the lengths of Ba–Ba and Hf–Ba bonds. Thus, the Ba–Ba bond length in the case of barium desorption from the barium crystal lattice (Fig. 9, a) is 4.56 Å. When a barium atom located on the surface of a barium crystal is desorbed, the Ba–Ba bond length is 4.59 Å (Fig. 9, b). At the same time, the Hf–Ba bond length is 2.91 Å in the case of desorption of a barium atom from a pure hafnium crystal lattice (Fig. 9, c) and 2.94 Å in desorption of a barium atom from a pure hafnium crystal lattice in the presence of another barium atom (Fig. 9, d). A zero energy value on the ordinate axis indicates the lack of interaction between the desorbed atom and the surface.

It follows from Fig. 9 that the detachment of a barium atom from a pure hafnium crystal lattice is the most energetically unfavorable option with an energy of 4.463 eV. Even a single additional barium atom present on the hafnium crystal surface reduces the desorption energy to 4.055 eV. If we consider the case of detachment of a barium atom from the crystal lattice of barium, the desorption energy is 1.657 eV; when the detached barium atom is positioned on the Ba crystal surface, the energy drops to 1.084 eV.

Thus, desorption of the upper layers of barium is energetically favorable compared to desorption of atoms from a hafnium crystal. As barium layers get removed with only 1–2 of them remaining on the hafnium surface, the detachment of barium atoms becomes less and less likely.

Conclusion

Molecular dynamics simulations with the use of the quantum-mechanical density functional method provided an opportunity to establish the patterns of interaction of adsorbed barium atoms with the crystal lattice of hexagonal hafnium, which is a film of five atomic layers, at a temperature of 800°C. It was found that the first few layers of barium atoms do not remain on the surface; instead, they diffuse into the hafnium film to a depth of several nanometers. Subsequent adsorbed layers of barium atoms accumulate on the surface, forming a crystalline barium film. The work function varied continuously in the course of these processes: the penetration of barium deep into hafnium raised the work function to 4.9 eV, while the formation of a crystalline barium film on the surface reduced the work function to the level typical of a 3D barium sample (3.74 eV).

It was established in the course of simulation that the work function of the structure reaches a plateau level of about 3.75 eV at the 23rd barium layer and remains virtually unchanged as the number of layers increases further to 30. Therefore, it is impractical to model more layers, and this number of layers may be considered optimal for obtaining high values of the work function and securing the anti-emission properties of grids.

Thus, it may be concluded that the thermionic emission from Hf grids with a hexagonal lattice structure used in pulsed vacuum tubes with a cathode-grid assembly with a dispenser cathode operating at a temperature of 1080°C is expected to be negligible due to high values of the

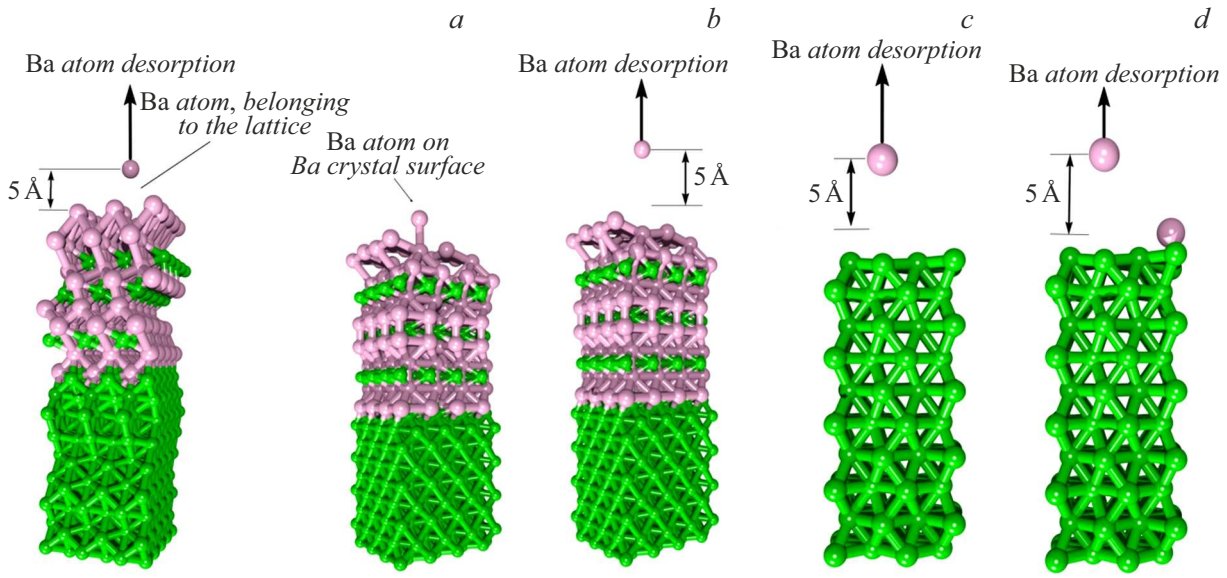

Figure 8. Desorption of barium from the crystal lattice of barium (*a*), desorption of a barium atom located on the surface of a barium crystal (*b*), desorption of a barium atom from a pure hafnium crystal lattice (*c*), and desorption of a barium atom from a pure hafnium crystal lattice in the presence of another barium atom (*d*).

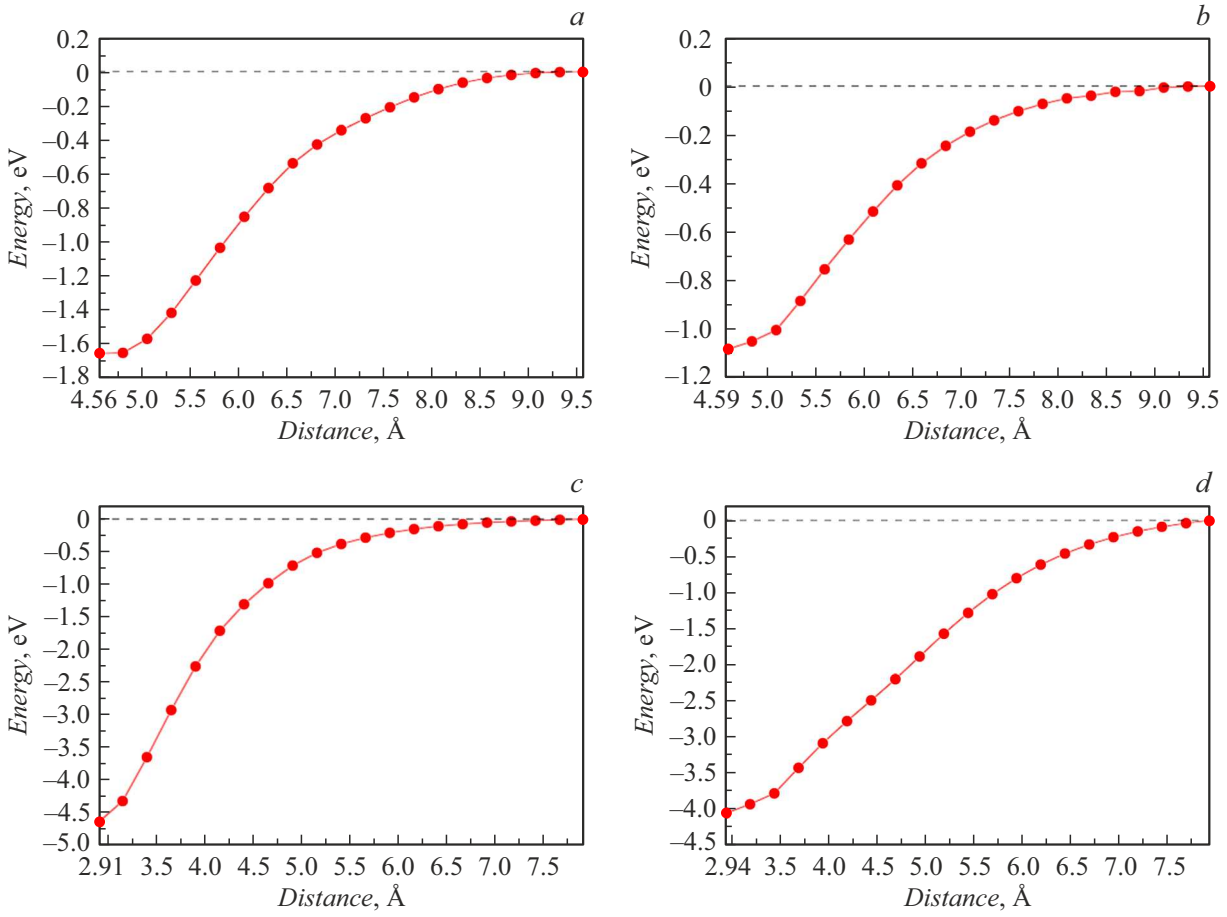

Figure 9. Desorption of barium from the crystal lattice of barium (*a*), desorption of a barium atom located on the surface of a barium crystal (*b*), desorption of a barium atom from a pure hafnium crystal lattice (*c*), and desorption of a barium atom from a pure hafnium crystal lattice in the presence of another barium atom (*d*).

electronic work function for the surface of hafnium with barium adsorbed on it.

Funding

This study was supported by a grant as part of the state assignment from the Ministry of Education and Science of the Russian Federation (project FSRR-2023-0008).

Conflict of interest

The authors declare that they have no conflict of interest.

References

[1] S.D. Zhuravlev, R.Yu. Bogachev, V.I. Rogovin, A.I. Petrosyan, V.I. Shesterkin, B.A. Grizbil, V.P. Ryabukho, A.A. Zakharov. Elektron. Tekh. Ser. 1, SVCh-Tekh., **4** (539), 45 (2018) (in Russian).
[2] S.D. Zhuravlev, V.I. Shesterkin. Tech. Phys., **64**, 1386 (2019) DOI: 10.1134/S1063784219090238
[3] R.Yu. Bogachev, V.V. Demin, S.D. Zhuravlev, T.M. Krachkovskaya, N.V. Rzhevin, V.I. Shesterkin. *Elektronnaya pushka moshchnoi impul'snoi LBV s dvoinymi setkami iz anizotropnogo piroliticheskogo grafita*. XIII Vserossiiskaya nauchno-tekhnicheskaya konferentsiya „Elektronika i mikroelektronika SVCh."Sbornik dokladov. SPb., May 27–31, 2024 (SPbGETU „LETI," SPb.), pp. 131–135 (in Russian).
[4] A.S. Gilmour Jr. Principles of Traveling Wave Tubes, (Artech House Publishers, 1994)
[5] J. Jiang, B. Jiang, C. Ren, T. Feng, Xi Wang, X. Liu, and S. Zou. J. Vacuum Sci. Technol. A, **23**, 506 (2005). DOI: 10.1116/1.1894726
[6] Electronic source. URL: https://www.icdd.com
[7] Electronic source. URL: https://www.crystallography.net
[8] Electronic source. URL: https://www.ill.eu/sites/fullprof
[9] A. García, N. Papior, A. Akhtar, E. Artacho, V. Blum, E. Bosoni, P. Brandimarte, M. Brandbyge, J.I. Cerdá, F. Corsetti, R. Cuadrado, V. Dikan, J. Ferrer, J. Gale, P. García-Fernández, V.M. García-Suá rez, S. García, G. Huhs, S. Illera, R. Korytár, P. Koval, I. Lebedeva, L. Lin, P. López-Tarifa, S.G. Mayo, S. Mohr, P. Ordejón, A. Postnikov, Y. Pouillon, M. Pruneda, R. Robles, D. Sánchez-Portal, J.M. Soler, R. Ullah, V. Wenzhe Yu, J. Junquera. J. Chem. Phys., **152** (20), 204108 (2020). DOI: 10.1063/5.0005077
[10] J.M. Soler, E. Artacho, J.D. Gale, A. García, J. Junquera, P. Ordejón, D. Sánchez-Portal. J. Phys. Condens. Matter., **14**, 2745 (2002). DOI: 10.1088/0953-8984/14/11/302
[11] J.E. Huheey, E.A. Keiter, R.L. Keiter. *Inorganic Chemistry: Principles of Structure and Reactivity* (HarperCollins College Publishers, NY., 1993)
[12] A.L. Allred. J. Inorganic and Nuclear Chem., **17** (3–4), 215 (1961). DOI: 10.1016/0022-1902(61)80142-5
[13] G.S. Rohrer. *Structure and Bonding in Crystalline Materials* (Cambridge University Press, 2001), p. 478. DOI: 10.1017/CBO9780511816116
[14] J. Jiang, B. Jiang, C. Ren, T. Feng, X. Wang, X. Liu, S. Zou. J. Vacuum Sci. Technol. A: Vacuum, Surfaces, and Films, **23** (3), 506 (2005). DOI: 10.1116/1.1894726

Translated by D.Safin